

Non-Newtonian effects in the peristaltic flow of a Maxwell fluid

David Tsiklauri^{1,*} and Igor Beresnev^{2,†}

¹*Space and Astrophysics Group, Department of Physics, University of Warwick, Coventry, CV4 7AL, United Kingdom*

²*Department of Geological and Atmospheric Sciences, Iowa State University, 253 Science I, Ames, Iowa 50011-3212*

(Received 10 January 2001; revised manuscript received 26 April 2001; published 29 August 2001)

We analyzed the effect of viscoelasticity on the dynamics of fluids in porous media by studying the flow of a Maxwell fluid in a circular tube, in which the flow is induced by a wave traveling on the tube wall. The present paper investigates phenomena brought about into the classic peristaltic mechanism by inclusion of non-Newtonian effects that are important, e.g., for hydrocarbons. This problem has numerous applications in various branches of science, including the stimulation of fluid flow in a porous media under the effect of elastic waves and studies of blood flow dynamics in living creatures. We have found that in the extreme non-Newtonian regime, there is a possibility of a fluid flow in the direction *opposite* to the propagation of the wave traveling on the tube wall.

DOI: 10.1103/PhysRevE.64.036303

PACS number(s): 47.55.Mh, 47.60.+i, 68.08.-p, 68.43.Pq

I. INTRODUCTION

Investigation of flow dynamics of a fluid in a tube having circular cross section, induced by a wave traveling on its wall (boundary), has many applications in various branches of science. The physical mechanism of the flow induced by the traveling wave can be well understood and is known as the so-called peristaltic transport mechanism. This mechanism is a natural cause of motion of fluids in the body of living creatures, and it frequently occurs in organs such as ureters, intestines, and arterioles. Peristaltic pumping is also used in medical instruments such as the heart-lung machine, etc. [1].

Laboratory experiments have shown that an external sonic radiation can considerably increase the flow rate of a liquid through a porous medium (Refs. [1,2] and references therein). Initially, the idea of flow stimulation via waves traveling on the flow boundary, in the context of porous media, has been proposed by Ganiev and collaborators [3]. They proposed that sonic radiation generates traveling waves on the pore walls in a porous medium. These waves, in turn, generate a net flow of fluid via the peristaltic mechanism. Later, this problem has been studied in a number of publications, where authors used different simplifying assumptions in order to solve the problem (see, e.g., Ref. [4]). The most recent and general study of the stimulation of fluid flow in porous media via peristaltic mechanism is presented in Ref. [1], which we will use as a starting point in order to include non-Newtonian effects into the peristaltic model.

It is clear that a usual peristaltic mechanism discussed, e.g., in Ref. [1] can be used to describe the behavior of a classic Newtonian fluid, however, e.g., oil and other hydrocarbons exhibit significant non-Newtonian behavior [5]. The aim of this paper is therefore, to incorporate non-Newtonian effects into the classical peristaltic mechanism [1]. Thus, the present paper formulates a realistic model of the peristaltic mechanism, which is applicable to the non-Newtonian fluids

(e.g., hydrocarbons) not only to the Newtonian ones (e.g., ordinary water) which have been extensively investigated in the past [1].

It should be noted that there were similar studies in the past (Ref. [6] and references therein). However, the previous contributions discussed the peristaltic mechanism for rheological equations other than the Maxwellian one. Thus, the present paper fills this gap in the literature. In addition, this paper is motivated by the recent results of del Rio, *et al.*, [7], and Tsiklauri and Beresnev [8], who found effects, including the enhancement of a *Maxwellian fluid* flow in a tube that was subjected to an oscillatory pressure gradient.

II. THE MODEL

We consider an axisymmetric cylindrical tube (pore) of radius R and length L . We assume that an elastic wave induces a traveling wave on the wall (boundary) of the tube with the displacement of the following form:

$$W(z,t) = R + a \cos\left[\frac{2\pi}{\lambda}(z - ct)\right], \quad (1)$$

where a is the amplitude of the traveling wave, while λ and c are its wavelength and velocity, respectively. We note that the z axis of the (r, ϕ, z) cylindrical coordinate system is directed along the axis of the tube.

The equations that govern the flow are the balance of mass

$$\frac{\partial \rho}{\partial t} + \vec{\nabla} \cdot (\rho \vec{v}) = 0, \quad (2)$$

and the momentum equation

$$\rho \frac{\partial \vec{v}}{\partial t} + \rho(\vec{v} \cdot \vec{\nabla})\vec{v} = -\vec{\nabla} p - \vec{\nabla} \cdot \tilde{\tau}, \quad (3)$$

where ρ , p , and \vec{v} are the fluid density, pressure, and velocity, respectively; $\tilde{\tau}$ represents the viscous stress tensor. We describe the viscoelastic properties of the fluid using Maxwell's model [7], which assumes that

*Email address: tsikd@astro.warwick.ac.uk

†Email address: beresnev@iastate.edu

$$t_m \frac{\partial \tilde{\tau}}{\partial t} = -\mu \vec{\nabla} \vec{v} - \frac{\mu}{3} \vec{\nabla} \cdot \vec{v} - \tilde{\tau}, \quad (4)$$

where μ is the viscosity coefficient and t_m is the relaxation time.

We further assume that the following equation of state holds:

$$\frac{1}{\rho} \frac{d\rho}{dp} = \kappa, \quad (5)$$

where κ is the compressibility of the fluid. We also assume that the fluid's velocity has only r and z components.

We make use of “no-slip” boundary condition at the boundary of the tube, i.e.,

$$v_r(W, z, t) = \frac{\partial W}{\partial t}, \quad v_z(W, z, t) = 0. \quad (6)$$

Equation (4) can be rewritten in the following form:

$$\left(1 + t_m \frac{\partial}{\partial t}\right) \tilde{\tau} = -\mu \vec{\nabla} \vec{v} - \frac{\mu}{3} \vec{\nabla} \cdot \vec{v}. \quad (7)$$

Further, we apply the operator $(1 + t_m \partial/\partial t)$ to the momentum equation (3) and eliminate $\tilde{\tau}$ in it using Eq. (7):

$$\begin{aligned} & -\left(1 + t_m \frac{\partial}{\partial t}\right) \vec{\nabla} p + \mu \vec{\nabla}^2 \vec{v} + \frac{\mu}{3} \vec{\nabla} (\vec{\nabla} \cdot \vec{v}) \\ & = \left(1 + t_m \frac{\partial}{\partial t}\right) \left[\rho \frac{\partial \vec{v}}{\partial t} + \rho (\vec{v} \cdot \vec{\nabla}) \vec{v} \right]. \end{aligned} \quad (8)$$

The equations are made dimensionless by scaling the length by R and time by R/c . Also, we have introduced the following dimensionless variables (and have omitted the tilde sign in the latter equations): $\tilde{W} = W/R$, $\tilde{\rho} = \rho/\rho_0$, $\tilde{v}_r = v_r/c$, $\tilde{v}_z = v_z/c$, and $\tilde{p} = p/(\rho_0 c^2)$. Here, ρ_0 is the regular (constant) density at the reference pressure p_0 . We have also introduced $\epsilon = a/R$, $\alpha = 2\pi R/\lambda$, $\text{Re} = \rho_0 c R/\mu$, and $\chi = \kappa \rho_0 c^2$.

Following Ref. [1], we seek the solution of the governing equations in a form

$$\begin{aligned} p &= p_0 + \epsilon p_1(r, z, t) + \epsilon^2 p_2(r, z, t) + \dots, \\ v_r &= \epsilon u_1(r, z, t) + \epsilon^2 u_2(r, z, t) + \dots, \\ v_z &= \epsilon v_1(r, z, t) + \epsilon^2 v_2(r, z, t) + \dots, \\ \rho &= 1 + \epsilon \rho_1(r, z, t) + \epsilon^2 \rho_2(r, z, t) + \dots. \end{aligned}$$

Then, doing a usual perturbative analysis using the latter expansions, we can obtain a closed set of governing equations for the first (ϵ) and second (ϵ^2) order.

Further, following the authors of Refs. [1,8], we seek the solution of the liner problem in the form

$$u_1(r, z, t) = U_1(r) e^{i\alpha(z-t)} + \bar{U}_1(r) e^{-i\alpha(z-t)},$$

$$v_1(r, z, t) = V_1(r) e^{i\alpha(z-t)} + \bar{V}_1(r) e^{-i\alpha(z-t)},$$

$$p_1(r, z, t) = P_1(r) e^{i\alpha(z-t)} + \bar{P}_1(r) e^{-i\alpha(z-t)},$$

$$\rho_1(r, z, t) = \chi P_1(r) e^{i\alpha(z-t)} + \chi \bar{P}_1(r) e^{-i\alpha(z-t)}.$$

Here and in the following equations, the bar denotes a complex conjugate.

On the other hand, we seek the second (ϵ^2) order solution in the form

$$u_2(r, z, t) = U_{20}(r) + U_2(r) e^{i2\alpha(z-t)} + \bar{U}_2(r) e^{-i2\alpha(z-t)},$$

$$v_2(r, z, t) = V_{20}(r) + V_2(r) e^{i2\alpha(z-t)} + \bar{V}_2(r) e^{-i2\alpha(z-t)},$$

$$p_2(r, z, t) = P_{20}(r) + P_2(r) e^{i2\alpha(z-t)} + \bar{P}_2(r) e^{-i2\alpha(z-t)},$$

$$\rho_2(r, z, t) = D_{20}(r) + D_2(r) e^{i2\alpha(z-t)} + \bar{D}_2(r) e^{-i2\alpha(z-t)}.$$

The latter choice of solution is motivated by the fact that the peristaltic flow is essentially a nonlinear (second-order) effect [1], and adding a nonoscillatory term in the first order gives only a trivial solution. Thus, we can add nonoscillatory terms, such as $U_{20}(r)$, $V_{20}(r)$, $P_{20}(r)$, and $D_{20}(r)$, which do not cancel out in the solution after the time averaging over the period, only in the second and higher orders.

In the first order by ϵ we obtain

$$\begin{aligned} & -(1 - i\alpha t_m) P_1' + \frac{1}{\text{Re}} \left(U_1'' + \frac{U_1'}{r} - \frac{U_1}{r^2} - \alpha^2 U_1 \right) \\ & + \frac{1}{3 \text{Re}} \frac{d}{dr} \left(U_1' + \frac{U_1}{r} + i\alpha V_1 \right) = -i\alpha (1 - i\alpha t_m) U_1, \end{aligned} \quad (9)$$

$$\begin{aligned} & -i\alpha (1 - i\alpha t_m) P_1' + \frac{1}{\text{Re}} \left(V_1'' + \frac{V_1'}{r} - \alpha^2 V_1 \right) \\ & + \frac{i\alpha}{3 \text{Re}} \left(U_1' + \frac{U_1}{r} + i\alpha V_1 \right) = -i\alpha (1 - i\alpha t_m) V_1, \end{aligned} \quad (10)$$

$$\left(U_1' + \frac{U_1}{r} + i\alpha V_1 \right) = i\alpha \chi P_1. \quad (11)$$

Here, the prime denotes a derivative with respect to r .

Further, we rewrite the systems (9)–(11) in the following form:

$$-\gamma P_1' + \left(U_1'' + \frac{U_1'}{r} - \frac{U_1}{r^2} - \beta^2 U_1 \right) = 0, \quad (12)$$

$$-\gamma P_1 - \frac{i}{\alpha} \left(V_1'' + \frac{V_1'}{r} - \beta^2 V_1 \right) = 0, \quad (13)$$

where

$$\gamma = (1 - i\alpha t_m) \text{Re} - i\alpha \chi / 3, \quad \beta^2 = \alpha^2 - i\alpha (1 - i\alpha t_m) \text{Re}. \quad (14)$$

Note, that Eqs. (12) and (13) are similar to Eq. (3.11) from Ref. [1], except that γ and β are modified by substitution $\text{Re} \rightarrow (1 - i\alpha t_m)\text{Re}$.

Repeating the analysis similar to the one from Ref. [1], we obtain the Master equation for $U_1(r)$ and find its general solution as

$$U_1(r) = C_1 I_1(\nu r) + C_2 I_1(\beta r), \quad (15)$$

where I_1 is the modified Bessel function of the first kind of order 1, and C_1 and C_2 are complex constants defined by

$$C_1 = \frac{\alpha \beta \nu i I_0(\beta)}{2[\alpha^2 I_0(\nu) I_1(\beta) - \beta \nu I_0(\beta) I_1(\nu)]},$$

$$C_2 = \frac{-\alpha^3 i I_0(\nu)}{2[\alpha^2 I_0(\nu) I_1(\beta) - \beta \nu I_0(\beta) I_1(\nu)]},$$

where

$$\nu^2 = \alpha^2 \frac{(1 - \chi)(1 - i\alpha t_m)\text{Re} - (4/3)i\alpha\chi}{(1 - i\alpha t_m)\text{Re} - (4/3)i\alpha\chi}.$$

Here, I_0 is the modified Bessel function of the first kind of order 0.

We also obtain the general solution for $V_1(r)$:

$$V_1(r) = \frac{i\alpha C_1}{\nu} I_0(\nu r) + \frac{i\beta C_2}{\alpha} I_0(\beta r).$$

The second-order solution $V_{20}(r)$ can also be found in a way similar to the one used in Ref. [1]:

$$V_{20}(r) = D_2 - (1 - i\alpha t_m)\text{Re} \int_r^1 [V_1(\zeta) \bar{U}_1(\zeta) + \bar{V}_1(\zeta) U_1(\zeta)] d\zeta,$$

where D_2 is a constant defined by

$$D_2 = -\frac{i\alpha C_1}{2} I_1(\nu) - \frac{i\beta^2 C_2}{2\alpha} I_1(\beta) + \frac{-i\alpha \bar{C}_1}{2} I_1(\bar{\nu}) + \frac{i(\beta^2 C_2)}{2\alpha} I_1(\bar{\beta}).$$

The net dimensionless fluid flow rate Q can be calculated as [1]

$$Q(z, t) = 2\pi \left[\epsilon \int_0^1 v_1(r, z, t) r dr + \epsilon^2 \int_0^1 v_2(r, z, t) r dr + O(\epsilon^3) \right].$$

In order to obtain the net flow rate averaged over one period of time, we have to calculate

$$\langle Q \rangle = \frac{\alpha}{2\pi} \int_0^{2\pi/\alpha} Q(z, t) dt.$$

This time averaging yields

$$\langle Q \rangle = 2\pi \epsilon^2 \int_0^1 V_{20}(r) r dr$$

or finally substituting the explicit form of $V_{20}(r)$, we obtain for the dimensionless net flow rate

$$\langle Q \rangle = \pi \epsilon^2 \left[D_2 - (1 - i\alpha t_m)\text{Re} \int_0^1 r^2 [V_1(r) \bar{U}_1(r) + \bar{V}_1(r) U_1(r)] dr \right]. \quad (16)$$

III. NUMERICAL RESULTS

In the previous section, we have shown that the inclusion of non-Newtonian effects into the classical peristaltic mechanism by using the Maxwell fluid model yields the following change: $\text{Re} \rightarrow (1 - i\alpha t_m)\text{Re}$ in all of the solutions.

It is known that the viscoelastic fluids, described by the Maxwell model, have different flow regimes depending on the value of the parameter $De = t_v/t_m$, which is called the Deborah number [7]. In effect, the Deborah number is a ratio of the characteristic time of viscous effects $t_v = \rho R^2/\mu$ to the relaxation time t_m . As noted in Ref. [7], the value of the parameter De (which the authors of Ref. [7] actually call α) determines in which regime the system resides. Beyond a certain critical value ($De_c = 11.64$), the system is dissipative, and conventional viscous effects dominate. On the other hand, for small De ($De < De_c$) the system exhibits viscoelastic behavior.

A numerical code has been written to calculate $\langle Q \rangle$ according to Eq. (16). In order to check the validity of our code, we run it for the parameters similar to the ones used by other authors. For instance, for $\epsilon = 0.15$, $\text{Re} = 100.00$, $\alpha = 0.20$, $\chi = 0$, and $t_m = 0$ we obtain $\langle Q \rangle = 0.2708706458$, which is equal (if we keep four digits after the decimal point) to the result of the authors of Ref. [1] who actually obtained $\langle Q \rangle = 0.2709$.

Further, we have made several runs of our code for different values of the parameter t_m . We note again that t_m enters the equations because we have included non-Newtonian effects into our model. Equation (16) will be identical to the similar Eq. (4.1) from Ref. [1] if we set $t_m = 0$ in all our equations.

The results of our calculation are presented in Fig. 1, where we investigate the dependence of $\langle Q \rangle$ on the compressibility parameter χ for the various values of t_m . In order to compare our results with the ones from Ref. [1], we have plotted $\langle Q \rangle$ for the following set of parameters: $\epsilon = 0.001$, $\text{Re} = 10000.00$, $\alpha = 0.001$, and $t_m = 0$ (solid line). We note that the curve is identical to the corresponding curve in Fig. 2 from Ref. [1]. This obviously corroborates the validity of our numerical code. Further, to investigate the dependence of the flow rate $\langle Q \rangle$ on t_m , we perform the calculation for a few values of t_m . When $t_m = 1.0$, we notice no noticeable change in the plot as both curves coincide within the plotting accuracy. For $t_m = 100.00$ (dashed curve with

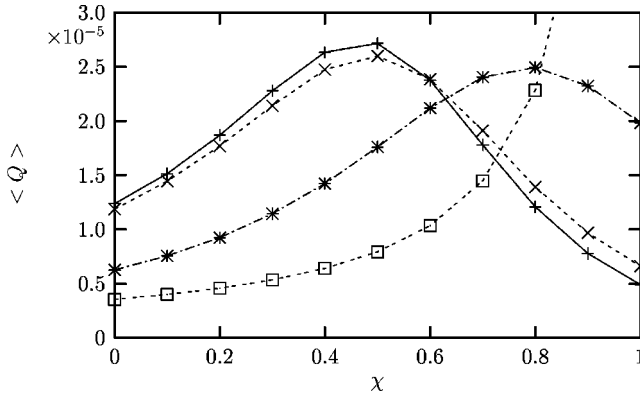


FIG. 1. Dimensionless flow rate $\langle Q \rangle$ as a function of compressibility parameter χ . The parameters used are $\epsilon=0.001$, $\text{Re}=10\,000.00$, and $\alpha=0.001$. $t_m=0$ corresponds to the solid line, whereas $t_m=100.00$, 1000.00 , and $10\,000.00$ correspond to the dashed curve with crosses, dash-dotted curve with asterisks, and dashed curve with empty squares, respectively.

crosses), we notice slight deviation from the Newtonian limiting case (solid line), which translates into shifting the maximum towards larger χ 's. For $t_m=1000.00$ (dash-dotted curve with asterisks), we notice further deviation from the Newtonian flow, which also translates into shifting the maximum towards larger χ 's. However, for $t_m=10\,000.00$ (dashed curve with empty squares), we note much more drastic changes, including the absence of a maximum and rapid growth of $\langle Q \rangle$ in the considered interval of variation of compressibility parameter χ . The observed pattern conforms to our expectation, since large t_m means small De ($De < De_c$) and the system exhibits strong viscoelastic behavior. Note that t_m is dimensionless and scaled by R/c .

After the above discussion, it is relevant to define quantitatively the transition point where the flow starts to exhibit (non-Newtonian) viscoelastic effects. It is known [7] that $De = t_v/t_m = (\rho R^2)/(\mu t_m)$. Now, using the definition of $\text{Re} = \rho c R/\mu$, we can define the critical value of t_m as

$$t_{mC} = \left(\frac{\text{Re}}{De_c} \right) \frac{R}{c}. \quad (17)$$

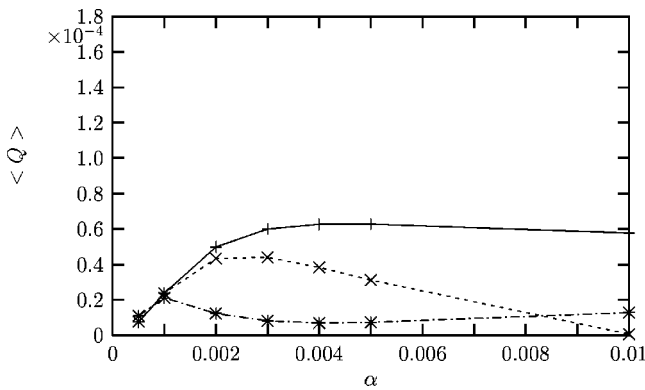


FIG. 2. Plot of dimensionless flow rate $\langle Q \rangle$ as a function of α . Here, $\epsilon=0.001$, $\text{Re}=10\,000.00$, and $\chi=0.6$. $t_m=0$ corresponds to the solid line, whereas $t_m=100.00$ and 1000.00 correspond to the dashed curve with crosses and dash-dotted curve with asterisks, respectively.

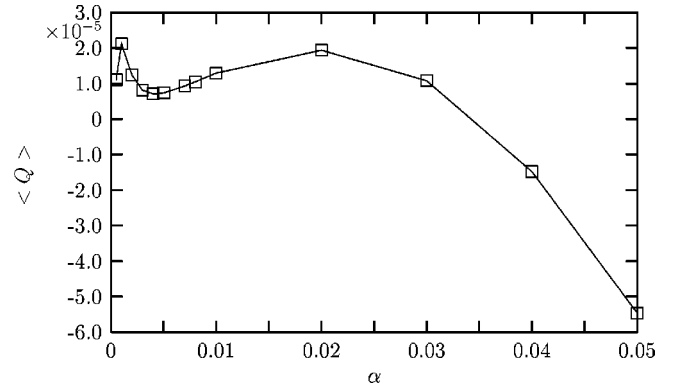


FIG. 3. Plot of dimensionless flow rate $\langle Q \rangle$ as a function of α on a larger (than in Fig. 2) interval of variation of α . Here, $\epsilon=0.001$, $\text{Re}=10\,000.00$, $\chi=0.6$, and $t_m=1000.00$.

In all our figures we have used $\text{Re}=10\,000.0$. If we put the latter value of Re and the critical value of the Deborah number 11.64 [7] into Eq. (17), we obtain $t_{mC}=859.11$ (measured in units of R/c). Therefore, the values of t_m greater than t_{mC} (for a given Re) correspond to subcritical ($De < De_c$) Deborah numbers for which viscoelastic effects are pronounced.

In Fig. 2 we investigate the behavior of the flow rate $\langle Q \rangle$ on the parameter α , which is the tube radius measured in wavelengths. Again, to check for the consistency of our numerical results with the ones from Ref. [1], and also investigate phenomena brought about by the introduction of non-Newtonian effects (appearance of nonzero relaxation time t_m) into the model, we first plot $\langle Q \rangle$ versus α for the following set of parameters: $\epsilon=0.001$, $\text{Re}=10\,000.00$, $\chi=0.6$, and $t_m=0$. If we compare the solid curve in our Fig. 2 with the dashed curve in Fig. 3 of Ref. [1], we will note no difference, which again corroborates the validity of our numerical code. We then set t_m to various nonzero values and investigate the changes introduced by non-Newtonian effects. As in Fig. 1, we notice no change for $t_m=1.0$. For $t_m=100.00$ and $t_m=1000.00$, we notice that the flow rate somewhat changes, attaining lower values as α (radius of the tube) increases.

We treat the latter, $t_m=1000.00$, case separately for the reason of an appearance of a effect of *negative* flow rates when the interval of variation of α is increased up to 0.05 . Again, we expect that for large t_m ($t_m > t_{mC}=859.11$), i.e., small De ($De < De_c$), the system should exhibit viscoelastic behavior. We note from Fig. 3 that for $\alpha \geq 0.035$, $\langle Q \rangle$ becomes *negative*, i.e., we observe backflow. In fact, by doing parametric studies we conclude that t_{mC} is the critical value of t_m , above which we observe backflow. By increasing t_m further, $t_m=10\,000.00$, we note from Fig. 4 that in this deeply non-Newtonian regime, $\langle Q \rangle$ becomes highly oscillatory, but what is unusual again is that we observe the negative flow rates for certain values of α , that is, the tube radius measured in wavelengths. Obviously, the negative $\langle Q \rangle$ means that flow occurs in the direction opposite to the direction of propagation of the traveling wave on the tube wall. Oscillatory behavior (appearance of numerous of maxima in the behavior of a physical variable) in the deeply non-

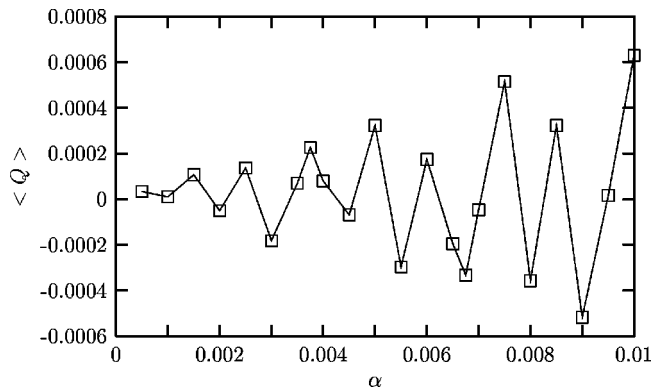


FIG. 4. Plot of dimensionless flow rate $\langle Q \rangle$ as a function of α . Here, $\epsilon=0.001$, $Re=10\,000.00$, $\chi=0.6$, and $t_m=10\,000.00$.

Newtonian regime is not new [8]. However, the flow of a fluid created by the peristaltic mechanism in the direction opposite to the direction of propagation of the traveling wave, is unusual and should be attributed to a complicated, nonlinear form of the response of a Maxwell fluid to the stress exerted by the wave.

IV. CONCLUSIONS

In this paper, we investigated the dynamics of fluid flow in a tube with a circular cross section, induced by a wave traveling on its wall (boundary). This problem has numerous applications in various branches of science, including stimulation of fluid flow in porous media under the effect of elastic waves.

The present paper investigates phenomena brought about into the classic peristaltic mechanism by the inclusion of non-Newtonian effects based on the model of a Maxwell fluid.

We have found that in the extreme non-Newtonian regime there is a possibility of flow in the direction opposite to the propagation of the wave traveling on the tube wall. A somewhat similar effect is known as the acoustic streaming [9], in which an acoustic wave propagating in a tube induces a mean flow in the direction of propagation in the acoustic boundary layer, but in the opposite direction in the central part of the tube. The mean flow or acoustic streaming is caused by the presence of friction at the bounding surfaces of the tube. While fluid away from the neighborhood of a boundary vibrates irrotationally as the acoustic wave passes, fluid in close proximity to the boundary must vibrate rotationally to satisfy the no-slip condition on the tube wall. This deviation from inviscid, irrotational behavior provides an effective driving force known as the Reynolds stress. This effective force, because of it is quadratic rather than linear, has a nonvanishing time-average tangential component to the tube wall that drives flow in the boundary layer. In the case considered in our paper, instead of having an acoustic wave propagating through the volume of the tube, we have a wave traveling on the tube wall; besides we have the further complication of considering non-Newtonian (Maxwell) fluid (recall that the discovered effect is demonstrated for the case of non-Newtonian regime $t_m/t_{mc} > 1.0$). Similarly, the peristaltic flow itself is a second-order nonlinear effect. Therefore, the flow of a fluid created by the peristaltic mechanism in the direction opposite to the direction of propagation of traveling wave (i.e., backflow) could be explained by a complicated, non-Newtonian, nonlinear response of a Maxwell fluid to the stress exerted by the traveling wave.

ACKNOWLEDGMENTS

This work was supported by the Iowa State University Center for Advanced Technology Development and ETREMA Products, Inc.

-
- [1] A.C.T. Aarts and G. Ooms, *J. Eng. Math.* **34**, 435 (1998).
 [2] I.A. Beresnev and P.A. Johnson, *Geophysics* **59**, 1000 (1994); T. Drake and I. Beresnev, *The American Oil and Gas Reporter*, September 1999, p. 101.
 [3] R.F. Ganiev, L.E. Ukrainskii, and K.V. Frolov, *Sov. Phys. Dokl.* **34**, 519 (1989).
 [4] A.H. Shapiro, M.Y. Jaffrin, and S.L. Weinberg, *J. Fluid Mech.* **37**, 799 (1969); F. Yin and Y.C. Fung, *J. Appl. Mech.* **36**, 579 (1969); S. Takabatake, K. Ayukawa, and A. Mori, *J. Fluid Mech.* **193**, 267 (1988).
 [5] C. Chang, Q.D. Nguyen, and H.P. Ronningsen, *J. Non-Newtonian Fluid Mech.* **87**, 127 (1999); B.P. Williamson, K. Walters, T.W. Bates, R.C. Coy, and A.L. Milton, *ibid.* **73**, 115 (1997); G.A. Nunez, G.S. Ribeiro, M.S. Arney, J. Feng, and D.D. Joseph, *J. Rheol.* **38**, 1251 (1994); L.T. Wardhaugh and D.V. Boger, *ibid.* **35**, 1121 (1991).
 [6] A.M. Siddiqui and W.H. Schwarz, *J. Non-Newtonian Fluid Mech.* **53**, 257 (1994).
 [7] J.A. del Rio, M.L. de Haro, and S. Whitaker, *Phys. Rev. E* **58**, 6323 (1998).
 [8] D. Tsiklauri and I. Beresnev, *Phys. Rev. E* **63**, 046304 (2001).
 [9] Q. Qi, R.E. Johnson, and J.G. Harris, *J. Acoust. Soc. Am.* **97**, 1499 (1995).